Artificial Spin Ice as an Interacting, Externally Driven Granular Material: Effective Temperature. [WORK IN PROGRESS]

Cristiano Nisoli and the Magnetic Mafia

July 10, 2009

Temperature is a single statistical parameter that fully describes a disordered state in thermal equilibrium. For athermal systems, like externally driven granular materials, where interaction energy scales greatly exceeds the traditional thermodynamic temperature, the large number of grains often warrant for statistical descriptions, and thus the notion of "effective temperatures" has been, often controversially, introduced theoretically [1], then extracted from simulations [2] and recently observed in experiments [3]. Here we extract a meaningful (and occasionally negative) effective temperature from athermal Artificial Spin Ice, demonstrate its predictive power and relate it to the external drive.

Artificial Spin Ice, a two-dimensional array of elongated single-domain permalloy islands whose shape anisotropy defines Ising-like spins arranged along the sides of a regular lattice, was recently engineered to study frustration-induced disorder [4]. Unlike other widely studied, naturally occurring frustrated materials [7, 8, 9, 10, 6, 11], Artificial Spin Ice can be imaged via Magnetic Force Microscopy (MFM), thus providing a powerful system which can be taylor-engineered to explore different geometries theoretical models. Indeed, the thermodynamics of 2-D ice systems has been widely studied - and often exactly solved - in the past four decades for a wide range of vertex models [12, 13, 14]. And yet ASI canot be considered in thermal equilibrium with the surroundings: interaction energies between islands are of the order of 10^5 K and temperature cannot induce spin-flipping fluctuations. Indeed each island ($80 \times 220 \times 25$ nm, with a magnetic moment $\sim 3 \times 10^7 \mu_B$) is a whole thermodynamic

Figure 1: **Square and Hexagonal Artificial Spin Ice**. From top to bottom: AFM and MFM of the two arrays; the 16 vertices of the square artificial ice and the 8 vertices of the hexagonal, their energy and multiplicity; the unique ground state of square ice and the degenerate ground state of hexagonal.[JIE, XIANGLIN, CAN YOU MAKE THIS FIGURE?]

system, like a grain in granular materials. However, as for grains, for which a successful extraction of an effective temperature has been recently reported [3], the large number of grains/islands involved suggests the viability of statistical treatments when fluctuations are activated via some sort of external drive. Similarly, Artificial Spin Ice is "externally driven" [4, 15, 16, 17]: in our experimental procedure it is subject to a rotating (at 1000 rpm) magnetic field, stepwise decreasing from 2000 Oe, far above Hc (770 Oe and independent of space) to zero with a constant step size, H_s after holding each step for 5 s. Different protocols correspond to different step-sizes ($H_s = 1.6, 3.2 \ldots 32$ Oe): previously reported data confirms our early heuristic intuition that smaller H_s would correspond to lower energies [16]. After demagnetization MFM images are taken, each containing a varying number of island (from one thousand to a few hundreds, depending on the size of the array). We report and interpret data of two different geometries, square and hexagonal (Figure 1), of varying sizes.

Following established approach [4, 17, 18] we describe our data within a vertex model [14]. Square ice we has 4 topologies for the 16 possible vertices, called Type I ... Type IV, of multiplicity $q_{\rm I} = 2$, $q_{\rm II} = 4$, $q_{\rm III} = 8$, $q_{\rm IV} = 2$, defined in Figure 1, corresponding to vertex energies $E_{\rm I}$, $E_{\rm II}$, $E_{\rm III}$ and fractional populations $n_{\rm I}$, $n_{\rm II}$, $n_{\rm III}$, $n_{\rm IV}$ (which can be extracted via MFM imaging), so that he specific vertex energy is $\overline{E} = E_{\rm I} n_{\rm I} + E_{\rm II} n_{\rm II} + E_{\rm III} n_{\rm III} + E_{\rm IV} n_{\rm IV}$. In Hexagonal Ice the vertex topologies are just two (Figure 1) of multiplicity $q_{\rm I} = 6$, $q_{\rm II} = 2$ and specific vertex energy $\overline{E} = E_{\rm I} n_{\rm I} + E_{\rm II} n_{\rm II}$. The two geometries imply completely different entropy vs. energy profiles for the vertex model: while square array posses an unique ground state of anti-ferromagnetic tiling of Type I vertices, in the Hexagonal an extensively degenerate tiling of Type I vertices returns significant residual entropy. Both allow ample regions of negative temperature as the higher energy configuration is completely ordered. Perhaps non surprisingly, they behave differently under AC demagnetization: while for square case the lower energy is never found, in the hexagonal case demagnetization returns the ground state and its excitations.

We extract a meaningful effective temperature from square Ice and use it to predict the widely different outcomes at different magnetic step-size and array sizes, by modeling the demagnetization protocol as a one-step non-equilibrium stochastic process at the vertex level – thus extending previous formalism [17]: the array starts completely polarized and during demagnetization the field carves types I, II, III or IV defects inside the polarized background, which is purely type-II. Without detailed knowledge of the kinetics, we ask ourselves what is the more likely outcome of such a process. In an isotropic, vertex-gas approximation, where each vertex is treated as an independent entity, there are $M = \frac{N!}{(N-D)! \prod_\alpha N_\alpha!}$ ways to tear D defects in the N vertices of a polarized tiling, allocated among the four vertex types with distribution N_α, $\alpha = {\rm I}, \ldots, {\rm IV}$. Calling $\rho = D/N$, $\nu_\alpha = N_\alpha/N$, we maximize $\ln M$ under an energy constraint on the defected vertices ensemble, or $\rho\sigma - \rho \ln \rho - (1-\rho) \ln (1-\rho) - \rho\beta_e \left(\sum_{\alpha={\rm I}}^{\rm IV} E_\alpha \nu_\alpha - E \right)$ – where $\sigma = -\sum_{\alpha={\rm I}}^{\rm IV} \nu_\alpha \ln \frac{\nu_\alpha}{q_\alpha}$ the entropy of the defected ensamble – thus obtaining a canonical distribution for the defects

$$\nu_\alpha = \frac{q_\alpha \exp\left(-\beta_e E_\alpha\right)}{Z(\beta_e)}, \tag{1}$$

as well as the expression for the auxiliary ρ

$$\rho\left(\beta_e\right) = \frac{1}{e^{-\sigma(\beta_e)} + 1}. \tag{2}$$

Eqs 1,2 provide the actual vertex populations as

$$\begin{array}{l} n_{\rm I} = \rho\nu_{\rm I}, \quad n_{\rm III} = \rho\nu_{\rm III}, \quad n_{\rm IV} = \rho\nu_{\rm IV} \\ n_{\rm II} = (1-\rho) + \rho\nu_{\rm II}. \end{array} \tag{3}$$

The reciprocal effective temperature $\beta_e = 1/{\rm T}_e$ can be extracted from an MFM scan via

$$\beta_e E_{\rm III} = \ln \frac{4\ n_{\rm I}}{n_{\rm III}}. \tag{4}$$

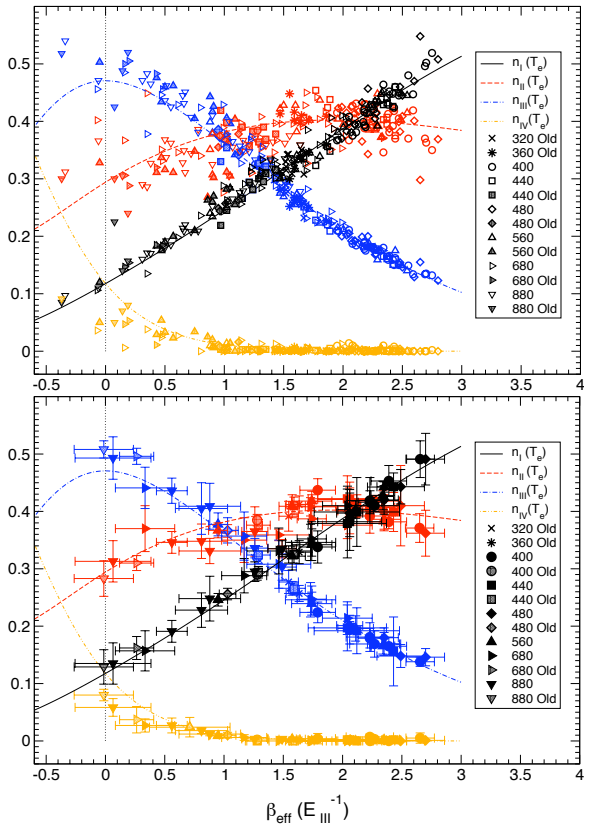

Figure 2: **Vertex Frequencies of Square Artificial Spin Ice vs. Effective Temperature:** experimental data from MFM images of arrays of different lattice constant and obtained at different H_s plotted against their effective reciprocal temperature β_e, along with theoretical lines. Top: each data reppresent an MFM image. Bottom: MFM image from the same array are averaged, errorbars shows fluctuations inside the same array. Note that older annealing protocol [4, 17] (open diamonds) returned substantially lower β_e.

We compute the vertex energies using a dumbbell model [19] for the magnetic dipole, considering only monopoles converging in each vertex: energies then scales as $(a-l)^{-1}$ and by imposing $E_{\rm I}=0$, $E_{\rm III}=1$ one finds $E_{\rm II}=\left(\sqrt{2}-1\right)/\left(\sqrt{2}-1/2\right)$ and $E_{\rm IV}=4\sqrt{2}/\left(2\sqrt{2}-1\right)$.

As we only can interrogate the array via small size MFM images, we can consider each of them as a subsistem of the larger lattice, thus expecting some large fluctuations. In the top panel of Figure 2 we plot experimental data of each MFM image for arrays of different sizes,*vs.* its extracted effective reciprocal temperature, along with the experimental prediction given by Equation 3. In the bottom panel we report average values of MFM images corresponding to the same array, along with their fluctuations (error bars report standard deviations of the mean for both temperature and population). Figure 2 shows that the effective temperature has a very good predictive power, effectively controlling the vertex populations for arrays of different size in different configurations, despite the crudity of the gas of vertices approximation. Indeed even data from older protocols fits very well – including larger arrays (560, 680, 880 nm) that could not be previously accounted for theoretically [17]. Larger sized arrays have larger fluctuations, as the number of vertices in the imaged subsystems (MFM scan) is much smaller. The underestimation of Type III at higher temperatures might be a signature of monopole attraction [19] among these vertices – which indeed appear in clusters - a feature that the current independent vertex approximation cannot describe. In an even more stringent test for our formalism, Figure 3-a reports the linear dependence between $\ln 5n_{\rm I}/2n_{\rm II}$ and $\ln 8n_{\rm I}/2n_{\rm III}$, which should correspond to the reciprocal effective temperatures $E_{\rm II}\beta_{e,{\rm II}}$ deduced from populations of Type II, and $E_{\rm III}\beta_{e,{\rm III}}$ deduced from Type III (we leave to the reader to check that at our effective temperatures, a purely canonical distribution with anomalous multiplicity of Type II equal to 5 instead than 4 provides a decent approximation). The linear fit returns an angular coefficient 0.441, very close to the expected theoretical value $E_{\rm II}/E_{\rm III}=\left(\sqrt{2}-1\right)/\left(\sqrt{2}-1/2\right)=0.453$; it also shows how further reduction of the stepsize will not lower temperature much more.

Is the effective temperature but a mathematical artifice, a Lagrangia multiplier, albeit useful to predict the thermodynamics of our system? Or does it - like the actual temperature does - in-

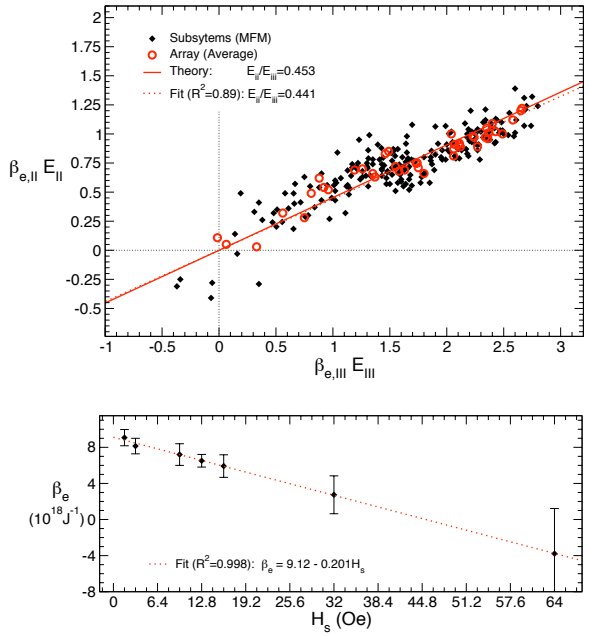

Figure 3: **Effective Temperature of Square Spin Ice.** Top: Extracted data $\ln 5n_{\rm I}/2n_{\rm II}$ plotted against $\ln 8n_{\rm I}/2n_{\rm III}$: linear fit returns a ratio of the two very close to the theoretical value. Bottom: Linear dependence of β_e as a function of the magnetic stepsize: β_e was obtained dividing data extracted valueln $\frac{4\ n_{\rm I}}{n_{\rm III}}$ by the estimated energy difference $\frac{2(\sqrt{2}-1)\mu_o}{4\pi}\frac{M^2}{L^2}\frac{1}{a} \simeq 1.4\ \frac{10^{-7}m}{a}\ 10^{-18}$ J.

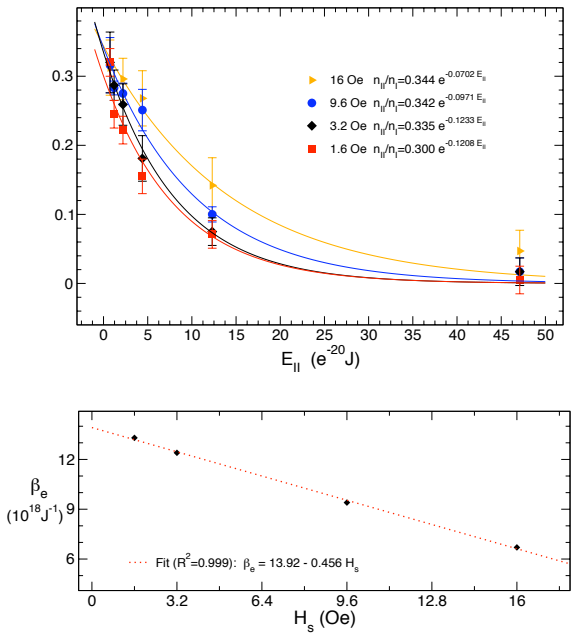

Figure 4: **Effective Temperature of Hexagonal Spin Ice.** Top: Exponential fits of $n_{\rm II}/n_{\rm I}$ vs. the energy $E_{\rm II}$; note the coefficient falling very close to the expected mutiplicity $q/3$. Bottom: Linear dependence of β_e as a function of the magnetic stepsize: β_e was obtained dividing data by linear fit of $\ln \frac{n_{\rm I}}{3n_{\rm II}}$ vs. the energy $E_{\rm II}$. Arrays os lattice constant $a = 650 \ldots 1620$ were used both in linear and exponential fit. Data for arrays of lattice constant 425 nm are reported in the top panel, although they were not used in the fitting, as its frequency of excitations is smaller than experimental error.

form us about the "effective bath" in which our system is merged, the external drive that fluidizes it? We can show that the effective temperature can be controlled via the external drive in a way strikingly analogous to that reported for vibro-fluidized granular materials [3]. Figure 3-b. shows the linear dependence of $< \beta_e >$ (averaged over the lattice constant a) in the magnetic step-size of the AC demagnetization. As we shall see soon, *this is not unique to the square geometry*. Incidentally, the reader should note the inclusion of higher step-size data (H_s =32, 64 Oe) in Figure 3 which, despite corresponding to non demagnetized arrays (residual magnetization up to 60 %), agrees very well with the linear fit in H_s. As the ratio $n_{\rm I}/n_{\rm III} = \nu_{\rm I}/\nu_{\rm III}$ does not depend upon ρ, we conclude that apparently defects are created in the most likely way by the external drive even though the latter is not capable to reach the maximize their number and thus ρ of Equation 2 does not equilibrate.

We test these concepts on a different geometrical array, the Hexagonal Ice. AC demagnetization, as mentioned before, very effectively returns the ground state of Hexagonal Spin Ice for arrays of small lattice constant (for a = 225, 260, 320, 425 nm the frequency of excitations is $\sim 10^{-3}$, below experimental error), and diluted excitations for larger lattice constant ($a = 650 \ldots 1620$ nm), thus making hexagonal ice a good candidate to study the dependence of effective temperature on array size and external magnetic field. As excita-

tions $n_{\rm II}$ completely defines the thermodynamics, the introduction of an effective temperature

$$\beta_e E_{\rm II} = \ln \frac{n_{\rm I}}{3n_{\rm II}} \qquad (5)$$

might seem only a re-parametrization with little predictive power. Nevertheless, when we extract $n_{\rm II}/n_{\rm I}$ from arrays of different size yet annealed at the same magnetic step H_s, and plot it against the respective energy $E_{\rm II}$ (obtained via micromagnetics, as we now study much larger lattices, we consider the full vertex interaction of dipole islands, instead of just the dumbbell tips that converge in the vertex) we find a remarkable exponential behaviour that suggests independence of the effective temperature from the size of the array. Figure 4-a shows these fits, from which we can extract the effective temperature β_e for each different magnetic step-size H_s, while the coefficient of the exponential is non surprisingly close to $q_{\rm II}/q_{\rm I} = 1/3$. Slightly better values of β_e are obtained via linear fit of Equation 5. Figure 4-b shows the remarkable linear dependence of these extracted $beta_e\beta_e$ from H_s, as also happens in the square case - although with different parameters: different geometries experience different effective temperature under the same magnetic drive.

Peter, could you add a conclusion? Peter, could you add a conclusion? Peter, could you add a conclusion? Peter, could you add a conclusion? Peter, could you add a conclusion? Peter, could you add a conclusion? Peter, could you add a conclusion? Peter, could you add a conclusion? All work and no play makes Jack a dull boy All work and no play makes Jack a dull boy All work and no play makes Jack a dull boy All work and no play makes Jack a dull boy All work and no play makes Jack a dull boy All work and no play makes Jack a dull boy ... now, where is the ax? Oh, here it is....

References

[1] Mehta and other review papers.

[2] H. A. Makse & J. Kurchan, Nature (London) **415** 614 (2002).

[3] G. D'Anna, P. Mayor, A. Barat, V. Loreto and Franco Nori, Nature (London) bf 424 909 (2003)

[4] R. F. Wang, C. Nisoli, R. S. Freitas, J. Li, W. McConville, B. J. Cooley, M. S. Lund, N. Samarth, C. Leighton, V. H. Crespi and P. Schiffer, Nature (London) **439**, 303 (2006).

[5] The magnetic moment of a single island, 80 $\times$ 220 $\times$ 25 nm thick, is $\sim 3 \times 10^7 \mu_B$.

[6] A. P. Ramirez in *Handbook of Magnetic Materials Vol. 13* (ed. K. J. H. Buschow) 423–520 (Elsevier Science, Amsterdam 2001).

[7] R. Moessner, Can. J. Phys. **79**, 1283 (2001).

[8] L. C. Pauling, J. Am. Chem. Soc. **57**, 2680 (1935); *The Nature of the Chemical Bond*, Cornell Univ. Press, Ithaca, NY (1945).

[9] M. J. Harris, S. T. Bramwell, D. F. McMorrow, T. Zeiske and K. W. Godfrey, Phys Rev. Lett. **79**, 2554 (1997).

[10] A. P. Ramirez, A. Hayashi, R. J. Cava, R. Siddharthan, and B. S. Shastry, Nature **399**, 333 (1999).

[11] S. T. Bramwell and M. J. P. Gingras, Science **294**, 1495 (2001).

[12] E. H. Lieb, Phys. Rev. Lett. **18**, 692 (1967).

[13] E. H. Lieb and F. W. Wu, in *Phase Transitions and Critical Phenomena*, vol. 1, C. Domb and M. S. Green, Eds. (Academic, London, 1971).

[14] R. Baxter, *Exactly Solved Models in Statistical Physics* (Academic, New York, 1982).

[15] R. F. Wang, J. Li, W. McConville, C. Nisoli, X. Ke, J. W. Freeland, V. Rose, M. Grimsditsch, P. Lammert, V. H. Crespi and P. Schiffer, J. Appl. Phys. (...)

[16] X. Ke (...)

[17] C. Nisoli, R. F. Wang, J. Li, W. McConville, P. H. Lammert, P. Schiffer and V. H. Crespi Phys. Rev. Lett. **98**, 217303 (2007).

[18] G. Möller and R. Moessner, Phys. Rev. Lett. **96**, 237202 (2006).

[19] C. Castelnovo, R. Moessner and S. L. Sondhi Nature **451** 42 (2008).